Lecture Notes in Physics 783

Elements of Numerical Relativity and Relativistic Hydrodynamics

From Einstein' s Equations to Astrophysical Simulations

Bearbeitet von
Carles Bona, Carlos Palenzuela-Luque, Carles Bona-Casas

1. Auflage 2009. Buch. xiv, 214 S. Hardcover
ISBN 978 3 642 01163 4
Format (B x L): 15,5 x 23,5 cm
Gewicht: 508 g

Chapter 2
The Evolution Formalism

2.1 Space plus time decomposition

The general covariant approach to general relativity is not adapted to our experience from everyday life. The most intuitive concept is not that of space-time geometry, but rather that of a time succession of space geometries. This 'flowing geometries' picture could be easily put into the computer, by discretizing the time coordinate, in the same way that the continuous time flow of the real life is coded in terms of a discrete set of photograms in a movie.

In this sense, we can say that general relativity theory, when compared with other physical theories like electromagnetism, has been built upside down. In Maxwell theory one starts with the everyday concepts of electric charges, currents, electric and magnetic fields. One can then write down a (quite involved) set of field equations, Maxwell equations, that can be easily interpreted by any observer. Only later some 'hidden symmetry' (Lorentz invariance) of the solution space is recognized, and this allows to rewrite Maxwell equations in a Lorentz-covariant form. But the price to pay is gluing charges and currents on one side, and electric and magnetic fields on the other, into new 4D objects that obscure the direct relation to experience the original (3D) pieces.

In general relativity, we have started from the top, at the 4D level, so we must go downhill, in the opposite sense:

- by selecting a specific (but generic) time coordinate;
- by decomposing every 4D object (metric, Ricci, and stress–energy tensors) into more intuitive 3D pieces;
- by writing down the (much more complicated) field equations that translate the manifestly covariant ones (1.26) in terms of these 3D pieces.

General covariance will then become a hidden feature of the resulting '3+1 equations.' The equations themselves will no longer be covariant under a general coordinate transformation. But, as the solution space is not being modified by the decomposition, general coordinate transformations will still

Bona, C. et al.: *The Evolution Formalism*. Lect. Notes Phys. **783**, 25–48 (2009)
DOI 10.1007/978-3-642-01164-1_2

map solutions into solutions (as it happens with Lorentz transformations in Maxwell equations). The underlying invariance of the equations under general coordinate transformations is then preserved when performing the 3+1 decomposition. General covariant 4D equations just show up this invariance in an explicit way.

2.1.1 A prelude: Maxwell equations

Maxwell equations are usually written as

$$\nabla \cdot \boldsymbol{E} = 4\pi q, \tag{2.1}$$

$$\nabla \cdot \boldsymbol{B} = 0, \tag{2.2}$$

$$-\partial_t \boldsymbol{E} + \nabla \times \boldsymbol{B} = 4\pi \boldsymbol{J}, \tag{2.3}$$

$$\partial_t \boldsymbol{B} + \nabla \times \boldsymbol{E} = 0, \tag{2.4}$$

where it is clear that the charge and current densities, q and $\boldsymbol{J}$, act as the sources of the electric and magnetic fields, $\boldsymbol{E}$ and $\boldsymbol{B}$. We assume here for simplicity the vanishing of both the electric and magnetic susceptibilities, so that $\boldsymbol{D} = \boldsymbol{E}$ and $\boldsymbol{B} = \boldsymbol{H}$.

The second pair of equations (2.3) and (2.4) can be interpreted as providing a complete set of time evolution equations for the electric and magnetic fields (evolution system), whereas the first two equations (2.1) and (2.2) do not contain time derivatives and can be interpreted then as constraints. A straightforward calculation shows that these constraints are first integrals of the evolution system, as a consequence of the charge continuity equation:

$$\partial_t \, q + \nabla \cdot \boldsymbol{J} = 0 \, . \tag{2.5}$$

Now, we can start joining pieces. The charge and current densities can be combined to form a four-vector I^μ,

$$I^\mu \equiv (q, \, \boldsymbol{J}) \, . \tag{2.6}$$

The electric and magnetic fields can be combined in turn to form an antisymmetric tensor, namely

$$F_{\mu\nu} \equiv \begin{pmatrix} 0 & -E_j \\ E_i & F_{ij} \end{pmatrix} , \qquad F_{ij} \equiv \epsilon_{ijk} B^k \tag{2.7}$$

(electromagnetic field tensor).

The pair (2.1) and (2.3) of Maxwell equations can then be written in the manifestly covariant form

$$\nabla_\nu \, F^{\mu\nu} = 4\pi \, I^\mu \, , \tag{2.8}$$

whereas the other pair (2.2) and (2.4) can be written as

$$\nabla_\rho F_{\mu\nu} + \nabla_\mu F_{\nu\rho} + \nabla_\nu F_{\rho\mu} = 0\,. \tag{2.9}$$

Note that, allowing for the antisymmetry of the electromagnetic tensor, the four-divergence of (2.8) leads immediately to the covariant version of the charge continuity equation (2.5), namely

$$\nabla_\mu I^\mu = 0\,. \tag{2.10}$$

This strongly reminds the general relativity situation, where Einstein's equations (1.26), allowing for the Bianchi identities (1.19), lead to the conservation of the stress–energy tensor.

2.1.2 Spacetime synchronization

Coming back to the general relativity case, the 3+1 spacetime decomposition is based on two main geometrical elements:

- The first one is the choice of a **synchronization**. This amounts to foliate spacetime by a family of spacelike hypersurfaces, so that any spacetime

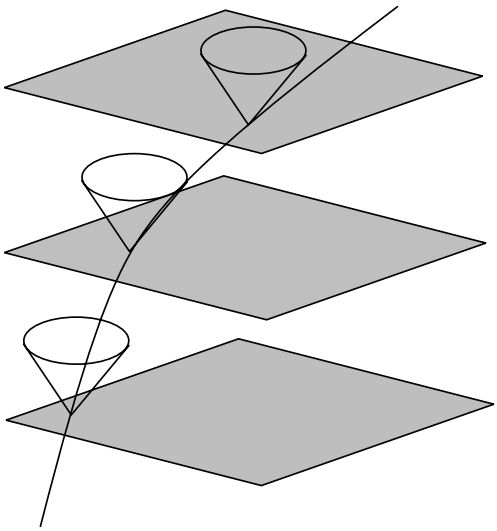

Fig. 2.1 The *time slicing* and one possible *time lines*, with some *light cones* drawn in order to show the causal character. The specific *time line* shown here starts being timelike, then changes to spacelike. The only requirement on *time lines* is that they cannot be tangent to the spacelike *slices:* they must 'thread' them. Note that, in this way, the slicing provides a natural choice of the affine parameter along time lines.

point belongs to one (and only one) slice. This geometrical construction can be easily achieved by selecting a regular spacetime function

$$\phi(x^\mu), \tag{2.11}$$

such that the level hypersurfaces of ϕ (defined by $\phi = \text{const}$) provide the desired foliation. In order to consider ϕ as a local time coordinate, we must make sure that the resulting slicing is spacelike, namely

$$g^{\mu\nu}\partial_\mu\phi\,\partial_\nu\phi < 0\,. \tag{2.12}$$

Every single slice can be considered as a 3D manifold. It is clear that curves on this manifold are also spacetime curves and therefore the spacetime metric can be directly used for measuring lengths on any 3D slice. In that way, the 3D metric γ_{ij} on every slice is induced by the spacetime metric $g_{\mu\nu}$. The overall picture can be easily understood by fully identifying the function ϕ with our time coordinate, that is,

$$\phi(x^\mu) \equiv t\,, \qquad \partial_\mu\phi = \delta^{(0)}_\mu\,, \tag{2.13}$$

so that the 3D line element

$$dl^2 = \gamma_{ij}\,dx^i dx^k \qquad (i,\,j = 1,2,3) \tag{2.14}$$

can be obtained from the 4D one by restricting it to the constant time surfaces, namely

$$\gamma_{ij} = g_{ij}\,. \tag{2.15}$$

- The second ingredient is the choice of a **congruence of time lines**. The simplest way is to get it as the integral curves of the system

$$\frac{dx^\mu}{d\lambda} = \xi^\mu\,, \tag{2.16}$$

so that the congruence is fully determined by the choice of the field of its tangent vectors ξ^μ. The affine parameter λ in (2.16) can be chosen to match the spacetime synchronization by imposing

$$\xi^\mu\partial_\mu\phi = 1\,. \tag{2.17}$$

Note that (2.17) is a very mild condition. It just requires that the time lines are not tangent to the constant time slices. It does not even demand the time lines to be timelike, in contrast with the stronger requirement (2.12) for the time slices (see Fig. 2.1).

Again, the meaning of (2.17) is more transparent if we use ϕ as the local time coordinate, that is (2.13),

$$\xi^\mu = \delta^\mu_{(0)}\,, \tag{2.18}$$

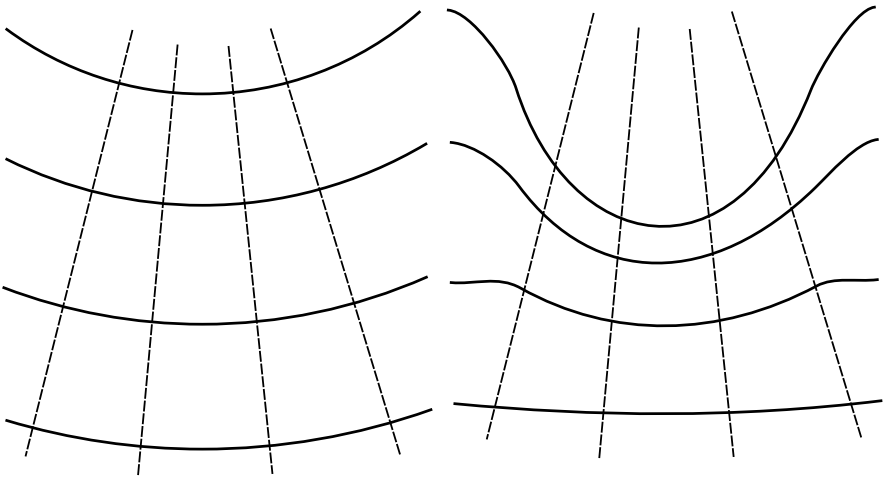

Fig. 2.2 Two different time foliations of the same spacetime. We see on the *left* a geodesic slicing. Coordinate time (represented by the *continuous level lines*) flows here homogeneously with the proper time along *normal (dashed) lines*, meaning that the lapse function is constant in this case. A coordinate singularity, the focusing of *normal lines*, is going to form in a finite coordinate time. We show in the *right side* a lapse function α such that proper time evolution slows down in the central region, while keeping a more uniform rate elsewhere. The *dashed lines* represent just the same freely falling observers, which are no longer normal to the constant time slices. This lapse-related degree of freedom will be of great help in numerical simulations of gravitational collapse, where we will like to slow down the proper time rate in the regions where a singularity is going to form (singularity avoidance).

so that the time lines equation (2.16) can be trivially integrated

$$x^0 = t \qquad x^i = \text{constant}. \tag{2.19}$$

We will focus first on the analysis of the time slicing. To do this, we will use normal coordinates, so that the time lines are chosen to be normal to the constant time slices. In this way we refrain from using the three extra degrees of freedom that would allow us to freely choose the tangent vector field ξ. Here we will not use any other ingredient than the slicing itself: we are restricting ourselves in this way to the simplest choice

$$\xi_\mu \sim \partial_\mu \phi \,, \tag{2.20}$$

or, in local adapted coordinates (2.13),

$$g_{0i} = 0 \tag{2.21}$$

(normal coordinates). The line element can then be written, allowing for (2.15) and (2.21), as

$$ds^2 = -\alpha^2 dt^2 + \gamma_{ij}\, dx^i dx^j \,, \tag{2.22}$$

where the factor α relates the coordinate time t with the proper time τ along the (normal) time lines:

$$d\tau = \alpha \, dt \, . \tag{2.23}$$

This means that the factor α (lapse function) gives us the rate at which proper time is elapsed along the normal lines (the time lines in normal coordinates).
Note that the lapse function can take different values at different spacetime points. This means that the amount of proper time elapsed when going from one slice to another can depend on the location. On the contrary, the amount of elapsed coordinate time is, by construction, independent of the space location. The particular case in which the lapse function α is constant corresponds to the geodesic slicing (see Fig. 2.2); the name will be justified in the next subsection. The combination of geodesic slicing plus normal space coordinates is known as the Gauss coordinate system.

2.1.3 The Eulerian observers

As stated before, in normal coordinates the congruence of time lines is provided by the slicing itself. We can view this congruence as the world lines of a field of observers which are at rest with respect to the spacetime synchronization (Eulerian observers). Their four-velocity field u^μ coincides, up to a sign, with the field of unit normals n^μ to the constant time slices

$$n_\mu = \alpha \, \partial_\mu \phi \qquad g^{\mu\nu} n_\mu n_\nu = -1 \, . \tag{2.24}$$

The relative sign comes from the normalization condition (2.17), that is,

$$u^\mu = -n^\mu \qquad u^\mu n_\mu = 1 \, . \tag{2.25}$$

In normal adapted coordinates, we have

$$u^\mu = \frac{1}{\alpha} \, \delta^\mu_{(0)} \, , \qquad n_\mu = \alpha \, \delta^{(0)}_\mu \, , \tag{2.26}$$

so that the tangent vector field u points forward in time.

The motion of any set of observers, represented by a congruence of time lines, can be decomposed into different kinematical pieces, namely

$$\nabla_\mu u_\nu = -u_\mu \dot{u}_\nu + \omega_{\mu\nu} + \chi_{\mu\nu} \, , \tag{2.27}$$

where every piece describes a different feature of the motion:

- **Acceleration**, described by the four-vector

$$\dot{u}_\mu \equiv u^\rho \nabla_\rho u_\mu \, . \tag{2.28}$$

It is the only non-trivial projection of (2.27) along u^μ.

- **Vorticity**, described by the antisymmetric tensor $\omega_{\mu\nu}$. It is the antisymmetric part of the projection of (2.27) orthogonal to u^μ ($\omega_{\mu\nu}u^\nu = 0$).
- **Deformation**, described by the symmetric tensor $\chi_{\mu\nu}$. It is the symmetric part of the projection of (2.27) orthogonal to u^μ ($\chi_{\mu\nu}u^\nu = 0$). It can be further decomposed into its trace, the expansion scalar

$$\theta \equiv tr(\chi)\,, \tag{2.29}$$

and its traceless part, the shear tensor

$$\sigma_{\mu\nu} = \chi_{\mu\nu} - \frac{\theta}{3}\,(g_{\mu\nu} + u_\mu u_\nu)\,. \tag{2.30}$$

In the case of the Eulerian observers, there is no vorticity because, by construction, they are orthogonal to the constant time hypersurfaces. Their motion is then characterized only by the acceleration vector and the deformation tensor. In adapted normal coordinates, allowing for (2.26), the acceleration vector is given by

$$\dot{u}_\mu = (0,\, \partial_i\, ln\alpha)\,, \tag{2.31}$$

so that the choice of a constant lapse corresponds to the inertial motion (free fall) of the Eulerian observers (this justifies the term 'geodesic slicing' we used in the previous subsection for the $\alpha =$ constant case).

The deformation tensor of the Eulerian observers consists also of space components only when written in adapted normal coordinates, namely,

$$\chi_{\mu\nu} = \begin{pmatrix} 0 & 0 \\ 0 & -K_{ij} \end{pmatrix}\,. \tag{2.32}$$

The 3D symmetric tensor K_{ij} in (2.32) is known as the extrinsic curvature of the slicing, whereas the minus sign in (2.32) arises from the sign convention (2.25).

The extrinsic curvature can be easily computed from (2.27). In normal adapted coordinates (2.26), we have

$$K_{ij} = -\frac{1}{2\alpha}\,\partial_t\,\gamma_{ij}\,. \tag{2.33}$$

Notice that K_{ij} admits then a double interpretation:

- From the time lines point of view, it provides the deformation $\chi_{\mu\nu}$ of the congruence of normal lines, as it follows from (2.27) and (2.32).
- From the slices point of view, it provides, up to a one half-factor, the Lie derivative of the induced metric γ_{ij} along the field of unit normals n^μ, as it follows from (2.26) and (2.33), and the space components of the 4D identity

$$\mathcal{L}_n(g_{\mu\nu}) = \nabla_\mu n_\nu + \nabla_\nu n_\mu\,. \tag{2.34}$$

Of course, these two points of view are equivalent, because the congruence of normal lines can be obtained from the slicing in a one-to-one way.

2.2 Einstein's equations decomposition

2.2.1 The 3+1 form of the field equations

Let us summarize the results of the previous section:

- We have decomposed the 4D line element into the 3+1 normal form (2.22), where the distinct geometrical meaning of the lapse function α and the induced metric γ_{ij} has been pointed out. This is analogous to decompose the electromagnetic tensor into its electric and magnetic field components.
- Einstein's field equations, contrary to Maxwell ones, are of second order. This means that one needs also to decompose the first derivatives of the 4D metric. We have started doing so in the previous subsection, where we have identified the pieces describing either the acceleration or the deformation tensor of the Eulerian observers (the lapse gradient and the extrinsic curvature K_{ij} of the slices). The remaining first derivatives can be easily computed in terms of the pieces we have got (see Table 2.1, where the full set of connection coefficients is displayed).

Table 2.1 The 3+1 decomposition of the 4D connection coefficients. Notice that the symbol $\widehat{\Gamma}^{\mu}_{\rho\sigma}$ stands for the connection coefficients of the 4D metric, whereas in what follows we will note as Γ^{k}_{ij} the connection coefficients of the induced 3D metric γ_{ij}.

$\widehat{\Gamma}^{0}_{00} = \partial_t\, ln(\alpha)$	$\widehat{\Gamma}^{k}_{00} = \alpha\gamma^{kj}\partial_j\,\alpha$
$\widehat{\Gamma}^{0}_{i0} = \partial_i\, ln(\alpha)$	$\widehat{\Gamma}^{k}_{i0} = -\alpha\gamma^{kj}K_{ij}$
$\widehat{\Gamma}^{0}_{ij} = -1/\alpha\, K_{ij}$	$\widehat{\Gamma}^{k}_{ij} = \Gamma^{k}_{ij}$

We have then for the moment a complete decomposition of the 'left-hand side' of the field equations. The corresponding decomposition of the source terms is just the well-known decomposition of the 4D stress–energy tensor $T_{\mu\nu}$ into parts which are either longitudinal (aligned with n_μ), transverse (orthogonal to n_μ), or of a mixed type, namely

- The **energy density**

$$\tau \equiv T^{\mu\nu} n_\mu n_\nu \tag{2.35}$$

- The **momentum density**

$$S_i \equiv T^{\mu}_{i} n_\mu \tag{2.36}$$

- The **stress tensor**

$$S_{ij} \equiv T_{ij}\,, \tag{2.37}$$

whose names arise from the physical interpretation that can be made from the point of view of the Eulerian observers.

Now we are in a position to translate the 4D field equations (1.26) in terms of the 3+1 quantities. We will reproduce here for clarity the equivalent (1.31) equations in terms of the 4D connection coefficients, so that we can apply the results of Table 2.1 in a straightforward way:

$$\partial_\rho \widehat{\Gamma}^\rho_{\mu\nu} - \partial_\mu \widehat{\Gamma}^\rho_{\rho\nu} + \widehat{\Gamma}^\rho_{\rho\lambda}\widehat{\Gamma}^\lambda_{\mu\nu} - \widehat{\Gamma}^\rho_{\lambda\mu}\widehat{\Gamma}^\lambda_{\rho\nu} = 8\pi\,(T_{\mu\nu} - \frac{1}{2}\,T^\lambda_\lambda\,g_{\mu\nu}). \tag{2.38}$$

The space components of (2.38) can then be written, after some algebra, as

$$\frac{1}{\alpha}\;\partial_t K_{ij} = -\frac{1}{\alpha}\;\nabla_i\alpha_j + R_{ij} - 2K^2_{ij} + trK\;K_{ij} - 8\pi\,[\,S_{ij} - \frac{1}{2}\,(trS - \tau)\;\gamma_{ij}\,]\,, \tag{2.39}$$

where the covariant derivatives and the Ricci tensor on the right-hand side are the ones obtained by considering every slice as a single 3D surface with metric γ_{ij} (traces are taken with the inverse matrix γ^{ij}). The same can be done with the mixed $(0i)$ components, namely

$$0 = \nabla_j\;(K_i{}^j - trK\;\delta_i{}^j) - 8\pi\,S_i\,, \tag{2.40}$$

where we get a first surprise: no time derivative appears on the left-hand side.

The remaining component of (2.38), the (00) one, leads in turn to

$$\frac{1}{\alpha}\;\partial_t\;trK = -\frac{1}{\alpha}\;\triangle\alpha + tr(K^2) + 4\pi\,(trS + \tau)\,. \tag{2.41}$$

This is also surprising, because the time derivative of the trace of K_{ij} can be obtained also from the space components equation (2.39). If we do so, we get by substituting the result into (2.41),

$$0 = tr\;R + (tr\;K)^2 - tr(K^2) - 16\pi\,\tau\,, \tag{2.42}$$

where again no time derivative appears, like in (2.40).

2.2.2 3+1 Covariance

General covariance is lost when decomposing the 4D field equations (2.38) into their 3+1 pieces ((2.39), (2.40), and (2.42)). If the solution space has not been changed in the process, general coordinate transformations still map solutions into solutions: the underlying invariance of the theory is intact. The

4D, general covariant version (2.38) just makes this underlying invariance manifest.

This does not mean, however, that covariance is completely lost. A closer look to the right-hand-side terms of the 3+1 system (2.39), (2.40), (2.41), and (2.42) shows that they are actually covariant under general space coordinate transformations

$$y^i = F^i(x^j, t)\,, \tag{2.43}$$

which preserve the geometry of every single slice. They are also unchanged under an arbitrary time coordinate rescaling

$$t' = G(t)\,, \tag{2.44}$$

which affects just the labeling of the slices, but not the slicing itself. We will call in what follows '3+1 covariance' the covariance under the restricted set of slicing-preserving coordinate transformations (2.43) and (2.44).

The 3+1 covariance of the right-hand sides of the system (2.39), (2.40), (2.41), and (2.42) follows from the fact that they are composed of two kinds of geometrical objects:

- 3D tensors, like the metric γ_{ij} or the Ricci tensor R_{ij}, which are intrinsically defined by the geometry of the slices, when considered as individual manifolds;
- pieces which can be obtained from 4D tensors by using the field of unit normals n_μ, which is intrinsically given by the slicing. This is the case of the three-acceleration $\partial_i\, ln\alpha$, the deformation (extrinsic curvature) K_{ij}, and the different projections of the stress–energy tensor.

This means that, in spite of the fact that we have used normal coordinates in their derivation, Eqs. (2.40) and (2.42) keep true in a generic coordinate system. Before getting a similar conclusion about the tensor equation (2.39), which contains a time derivative, let us consider the case of the simpler scalar equation (2.41). We know from the previous arguments that the right-hand side term will behave as a 3+1 scalar. We will consider now the transformation properties of the time derivative in the left-hand side step by step:

- It transforms under (2.43) as

$$\left(\frac{\partial\, trK}{\partial\, t}\right)_{x=\text{const}} = \left(\frac{\partial\, trK}{\partial\, t}\right)_{y=\text{const}} - \beta^k \left(\frac{\partial\, trK}{\partial\, y^k}\right)_{t=\text{const}}\,, \tag{2.45}$$

  where we have introduced the shift β^k:

$$\beta^k(y,t) \equiv \left(\frac{\partial\, y^k}{\partial\, x^r}\right)\left(\frac{\partial\, x^r}{\partial\, t}\right)_{y=\text{const}}\,. \tag{2.46}$$

- Concerning the time rescaling (2.44), let us notice that the lapse function is not a 3+1 scalar. It follows from its very definition (2.22) that it will transform instead as

$$\alpha' = \alpha \left(\frac{\partial t}{\partial t'} \right) , \tag{2.47}$$

so that the combination

$$\frac{1}{\alpha} \partial_t \tag{2.48}$$

is preserved. Note that the rescaling factor in (2.47) is independent of the space coordinates, so that the three-acceleration $\partial_i ln\alpha$ transforms as a 3+1 vector, as expected.

Putting these results together, it follows that the generic coordinate form of Eq. (2.41) can be obtained from their expression in normal coordinates by the following replacement:

$$\frac{1}{\alpha} \partial_t \, trK \quad \rightarrow \quad \frac{1}{\alpha} \left(\partial_t - \beta^k \partial_k \right) trK \, . \tag{2.49}$$

The 3+1 covariance of the resulting expression is clear if we notice that it has the intrinsic meaning of 'taking the proper time derivative of trK along the normal lines,' no matter what is our coordinate system. The same idea can lead to the corresponding generalization of the tensor equation (2.39), or any other in 3+1 form, by using as a rule of thumb the generic replacement

$$\frac{1}{\alpha} \partial_t \quad \rightarrow \quad \frac{1}{\alpha} \left(\partial_t - \mathcal{L}_\beta \right) . \tag{2.50}$$

2.2.3 Generic space coordinates

It follows from the previous considerations that the full set of Einstein's field equations can be decomposed in a generic coordinate system as follows:

$$\frac{1}{\alpha} \left(\partial_t - \mathcal{L}_\beta \right) \gamma_{ij} = -2K_{ij} \tag{2.51}$$

$$\frac{1}{\alpha} \left(\partial_t - \mathcal{L}_\beta \right) K_{ij} = -\frac{1}{\alpha} \nabla_i \alpha_j + R_{ij} - 2K_{ij}^2 + trK \, K_{ij} - 8\pi \left[S_{ij} - \frac{1}{2} \left(trS - \tau \right) \gamma_{ij} \right] \tag{2.52}$$

$$0 = \nabla_j \left(K_i{}^j - trK \, \delta_i{}^j \right) - 8\pi \, S_i \tag{2.53}$$

$$0 = tr \, R + (tr \, K)^2 - tr(K^2) - 16\pi \, \tau \, . \tag{2.54}$$

A simpler version, in Gauss coordinates ($\alpha = 1$, $\beta = 0$), was obtained by Darmois [1]. The normal coordinates version (2.39), (2.40), (2.41), and (2.42) is due to Lichnerowicz [2]. It was extended to the general case, although in the tetrad formalism, by Choquet-Bruhat [3]. See [4] for an interesting historical review.

Table 2.2 Same as Table 2.1 for the generic coordinates case. The symbol ∇ stands here for the covariant derivative with respect to the induced metric γ_{ij}.

$\widehat{\Gamma}^0_{00} = (\partial_t\alpha + \beta^k\alpha_k - K_{ij}\beta^i\beta^j)/\alpha$	$\widehat{\Gamma}^0_{i0} = (\partial_i\,\alpha - K_{ij}\beta^j)/\alpha$
$\widehat{\Gamma}^k_{00} = \gamma^{kj}[\partial_t\beta_j + \alpha\,\alpha_j - 1/2\,\partial_j(\gamma_{rs}\beta^r\beta^s)] - \beta^k\widehat{\Gamma}^0_{00}$	$\widehat{\Gamma}^k_{ij} = \Gamma^k_{ij} - \beta^k\widehat{\Gamma}^0_{ij}$
$\widehat{\Gamma}^k_{i0} = -\alpha\,K_i{}^k + \nabla_i\beta^k - \beta^k\widehat{\Gamma}^0_{i0}$	$\widehat{\Gamma}^0_{ij} = -1/\alpha\,K_{ij}$

Let us note, however, that 3+1 decompositions became popular from the work of Arnowitt, Deser, and Misner (ADM) about the Hamiltonian formalism [5], and they are often referred to as ADM equations for that reason, although the version appearing in [5] is an equivalent system in which the extrinsic curvature K_{ij} is replaced by the 'conjugate momentum' combination

$$\Pi_{ij} = K_{ij} - trK\,\gamma_{ij} \tag{2.55}$$

as a basic dynamical object. We will refer instead to (2.51), (2.52), (2.53), and (2.54) as the 3+1 field equations, emphasizing in this way the purely geometrical aspects of this approach.

The time-dependent space coordinates transformation (2.43), when applied to the line element (2.22), transforms it to the general form

$$ds^2 = -\alpha^2 dt^2 + \gamma_{ij}\,(dy^i + \beta^i dt)\,(dy^j + \beta^j dt)\,, \tag{2.56}$$

where it is clear that the new time lines $y =$ constant are no longer orthogonal to the constant time slices (see Fig. 2.3). The decomposition (2.56) is actually the most general one, where the four-coordinate degrees of freedom are represented by the lapse α and the shift β^k, whereas the normal coordinates form (2.22) is recovered only in the vanishing shift case.

Using a non-zero shift is certainly a complication. For instance, the inverse matrix of the 4D metric is given by

$$\hat{g}^{00} = -\frac{1}{\alpha^2}\,, \quad \hat{g}^{0i} = \frac{1}{\alpha^2}\,\beta^i\,, \quad \hat{g}^{ij} = \gamma^{ij} - \frac{1}{\alpha^2}\,\beta^i\,\beta^j\,, \tag{2.57}$$

and the connection coefficients contain now much more terms (see Table 2.2).

There are physical situations, however, in which a non-zero shift can be very convenient, for instance:

- When rotation is an important overall feature (spinning black holes, binary systems, etc.). If we want to adapt our time lines to rotate with the bodies, then we cannot avoid vorticity and normal coordinates can no longer be used. The shift choice will be then dictated by the overall motion of our system, so that our space coordinates will rotate with the bodies (co-rotating coordinates).

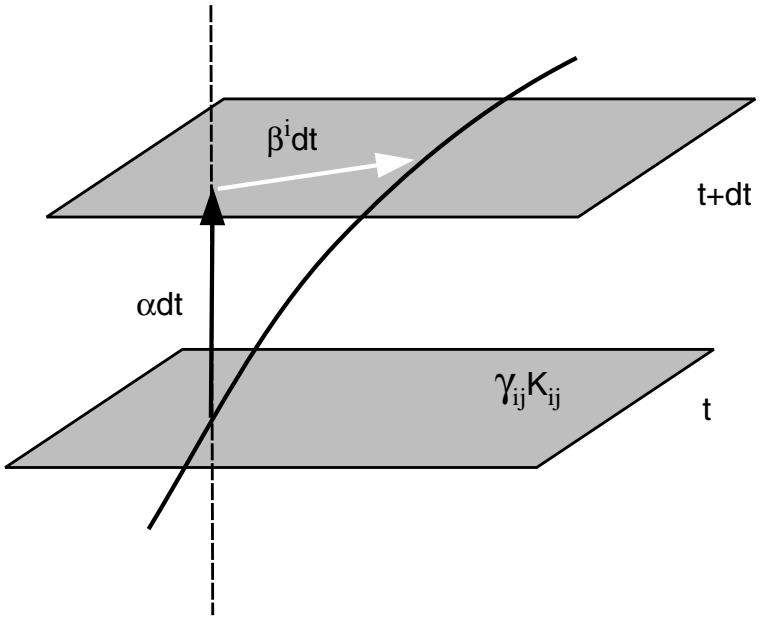

Fig. 2.3 Starting from a given *time slice*, we show the *normal line* (*dashed*) and the *time line* (*continuous*) passing through a given point. The lapse function provides the amount of proper time elapsed when moving to the next *time slice* along the *normal lines*. The shift measures the deviation between these *normal lines* and the actual *time lines* in the process.

- When one needs to use spacelike ('tachyon') time lines. As discussed before, this is allowed provided that the constant time slices remain spacelike. But one cannot have both things in normal coordinates: the squared norm of the vector $\xi^\mu = \delta^\mu_0$, tangent to the time lines, is given by

$$\xi \cdot \xi = -\alpha^2 + \gamma_{rs}\,\beta^r \beta^s\,, \tag{2.58}$$

  so that one would need a superluminal shift to do the job, namely

$$|\beta| > \alpha\,. \tag{2.59}$$

The use of a superluminal shift is mandatory if we want to move a black hole across the numerical domain [6]. This is not just a curiosity: it is rather the cornerstone in the 'moving puncture' approach, currently used in binary black hole simulations [7, 8]. It can also be very useful when performing numerical simulations in the vicinity of a black hole, if we want to prevent the horizon from growing too fast, enclosing all of our numerical grid before we have enough time to properly study the exterior region [9–11]. This is also a key ingredient in current binary black hole simulations based on the generalized harmonic formalism [12].

2.3 The evolution system

2.3.1 Evolution and constraints

The 3+1 decomposition (2.51), (2.52), (2.53), and (2.54) splits Einstein's field equations into two subsets of equations of a different kind:

- **Evolution equations**. These govern the time evolution of the basic dynamical fields $\{\gamma_{ij}\,,\ K_{ij}\}$, that is, (2.51) and

$$(\partial_t - \mathcal{L}_\beta)\ K_{ij} = -\nabla_i\,\alpha_j + \alpha\,[R_{ij} - 2K_{ij}^2 + trK\ K_{ij}\,] \\ - 8\pi\alpha\,[\,S_{ij} - \frac{1}{2}\,(trS - \tau)\,\gamma_{ij}\,]\,, \qquad (2.60)$$

  where, as stated before, no evolution equation is provided for any of the kinematical (coordinate gauge) fields $\{\alpha\,,\ \beta^i\}$.
- **Energy and momentum constraints**. These are constraints on the extrinsic curvature components K_{ij} and their space derivatives:

$$\mathcal{E} \equiv \frac{1}{2}\,[\,tr\,R + (tr\,K)^2 - tr(K^2)\,] - 8\pi\,\tau = 0 \qquad (2.61)$$

$$\mathcal{M}_i \equiv \nabla_j\,(K_i{}^j - trK\ \delta_i{}^j) - 8\pi\,S_i = 0\,. \qquad (2.62)$$

  The names of energy and momentum correspond to the matter terms appearing in each equation.

Note that we can always re-combine the equations, leading to different partitions of the full system. The constraint subset (2.61) and (2.62), however, can be univocally characterized as the one in which no time derivative of K_{ij} appears. This is not the case of the evolution subset: the one we have got in (2.60) will be called 'Ricci evolution system,' because it corresponds to the space components of the 4D Ricci tensor, as it was obtained in (2.39). One can use the energy constraint (2.61) to cancel out the energy density τ contribution in (2.60), so that the evolution subsystem will consist now in (2.51) plus

$$(\partial_t - \mathcal{L}_\beta)\ K_{ij} = -\nabla_i\,\alpha_j + \alpha\,[\,R_{ij} - 2K_{ij}^2 + trK\ K_{ij} - 8\pi\,S_{ij}\,] \\ -\frac{\alpha}{4}\,[\,tr\,R + (tr\,K)^2 - tr(K^2) - 16\pi\,trS\,]\,\gamma_{ij}\,. \qquad (2.63)$$

The subset (2.51) and (2.63) will be called Einstein evolution system, because it can be obtained from the space components of the 4D Einstein tensor, as can be easily seen from the matter terms appearing there. Although the Ricci and the Einstein evolution systems are not equivalent when considered independently, the complete set formed by any of them plus the energy and momentum constraints is the same one, the individual equations being just combined in different ways. We will make use of this recombination freedom in what follows.

2.3.2 Constraints conservation

A first look at the 3+1 version ((2.60), (2.61), and (2.62)) of the field equations shows its strong resemblance to the non-covariant form ((2.1), (2.2), (2.3), and (2.4)) of Maxwell equations, where there is also a subset of evolution equations ((2.3) and (2.4)) for the basic dynamical fields $\{\boldsymbol{E}, \boldsymbol{B}\}$ and a subset of constraints ((2.1) and (2.2)) on their space derivatives. The question arises whether the time derivative of the constraints, allowing for the evolution equations, would lead to new constraints. In the case of Maxwell equations, one can easily verify that this is not the case by taking the time derivatives of (2.1) and (2.2) and using both the evolution equations (2.3) and (2.4) and the charge conservation equation (2.5). This means that the constraints are first integrals of the full evolution system: they are preserved during time evolution. The 4D version of Maxwell equations (2.8) and (2.9) gives us the key to understand this result: both sides are conserved. The left-hand side is conserved by the antisymmetry of the electromagnetic field tensor $F^{\mu\nu}$, whereas the conservation of the right-hand side amounts to that of the charge-current four-vector J^{μ} (2.10).

In the case of the Einstein equations, the straightforward procedure of taking the time derivatives of the constraints (2.61) and (2.62) and then using the evolution equations (2.60) is impractical, even using an algebraic computing program. One can, however, take advantage of the lesson learned in the Maxwell case and look instead to the 4D form of the field equations (1.26), where again we find that both sides are conserved. The Einstein tensor $G^{\mu\nu}$ on the left-hand side is conserved due to the contracted Bianchi identities (1.19), whereas the conservation of the right-hand side amounts to that of the stress–energy tensor $T^{\mu\nu}$ (1.25). This is the idea that we advanced in the previous chapter, when discussing (1.29).

We will address here this point in more detail. Let us start by deriving the 3+1 version of (1.25). The most convenient way is to follow the standard procedure, that is,

- by computing it first in normal coordinates;
- by expressing the results in terms of 3+1 covariant quantities;
- by using then the standard replacement (2.50) to get the general expression, valid in any coordinate system.

We give just the final result for the stress–energy tensor conservation:

$$\frac{1}{\alpha}\left(\partial_t - \mathcal{L}_\beta\right)\tau + \nabla_j S^j = \tau\, trK - 2\, S^j\, \partial_j\, ln\alpha + K_{ij}\, S^{ij} \tag{2.64}$$

$$\frac{1}{\alpha}\left(\partial_t - \mathcal{L}_\beta\right) S_i + \nabla_j S_i{}^j = S_i\, trK - S_i{}^j\, \partial_j\, ln\alpha - \tau\, \partial_i\, ln\alpha\,, \tag{2.65}$$

which is the 3+1 version of the general covariant equation (1.25) (remember that all the indices are raised and lowered here with the induced metric γ_{ij}).

In the same way, we can also translate into the 3+1 language the corresponding conservation equation (1.29) for the difference between the left-hand side and the right-hand side of Einstein's field equations. Allowing for (2.61) and (2.62), we get

$$\frac{1}{\alpha}\left(\partial_t - \mathcal{L}_\beta\right)\,\mathcal{E} + \nabla_j\,\mathcal{M}^j = \mathcal{E}\;trK - 2\,\mathcal{M}^j\,\partial_j\,ln\alpha + K_{ij}\,\mathcal{P}^{ij} \tag{2.66}$$

$$\frac{1}{\alpha}\left(\partial_t - \mathcal{L}_\beta\right)\,\mathcal{M}_i + \nabla_j\,\mathcal{P}_i{}^j = \mathcal{M}_i\,trK - \mathcal{P}_i{}^j\,\partial_j\,ln\alpha - \mathcal{E}\,\partial_i\,ln\alpha\,, \tag{2.67}$$

where we have noted

$$\mathcal{P}_{ij} \equiv G_{ij} - 8\pi\,T_{ij}\,. \tag{2.68}$$

Now we can see how any eventual deviation from the energy and momentum constraints $\{\,\mathcal{E}\,,\mathcal{M}_i\}$ would propagate, assuming that the time evolution is given by the Einstein system (2.63):

$$\mathcal{P}_{ij} = 0 \tag{2.69}$$

$$\frac{1}{\alpha}\left(\partial_t - \mathcal{L}_\beta\right)\,\mathcal{E} + \nabla_j\,\mathcal{M}^j = \mathcal{E}\;trK - 2\,\mathcal{M}^j\,\partial_j\,ln\alpha \tag{2.70}$$

$$\frac{1}{\alpha}\left(\partial_t - \mathcal{L}_\beta\right)\,\mathcal{M}_i = \mathcal{M}_i\,trK - \mathcal{E}\,\partial_i\,ln\alpha\,. \tag{2.71}$$

The corresponding result for the Ricci evolution equation (2.60) can be obtained in an analogous way, by substituting the corresponding condition

$$\mathcal{P}_{ij} = \mathcal{E}\;\gamma_{ij} \tag{2.72}$$

into the full system (2.66) and (2.67). Independent of the choice, the resulting expression will be a linear homogeneous system on $\{\,\mathcal{E}\,,\mathcal{M}_i\}$, so that our statement that the vanishing of such quantities provides a set of first integrals of the evolution equations holds true, as anticipated from the 4D version (1.29).

2.3.3 Evolution strategies

The structure of the 3+1 field equations (2.60), (2.61), and (2.62) is so similar to that of the Maxwell equations (2.1), (2.2), (2.3), and (2.4) that one can get some inspiration for the equation-solving strategies in electromagnetism in order to do the same in the gravitational case. One can start by solving the constraint equations (2.61) and (2.62) to compute up to four of the six dynamical degrees of freedom (represented here by the components of the extrinsic curvature K_{ij}). When the constraints are first integrals of the

evolution system, the evolution equations (2.60) can be used later for computing the two remaining dynamical degrees of freedom.

This 'constrained evolution' approach is specially convenient in astrophysical scenarios where the general relativistic effects can be described as lower order corrections to the Newtonian gravity ones. This is because Newtonian gravity is completely analogous to electrostatics, in the sense that the time evolution of the fields is not provided by the equations. The constraints (2.61) and (2.62) contain then all the Newtonian effects whereas genuine relativistic effects, like the field dynamics leading to gravitational waves, must be found instead in the evolution subset (2.60). One could say that the constraints contain all the dynamical degrees of freedom, apart from the two of them corresponding to gravitational radiation and the ones related with the coordinate gauge freedom, as we will justify later.

From the numerical relativity point of view, the constrained evolution approach, although it can be useful to deal with specific physical situations, is not very convenient for building a general purpose code. There are many reasons for this:

- Constraint equations (2.61) and (2.62) are of elliptic type (exemplified by the Laplace equation). This means that particular solutions are of a non-local nature: they depend strongly on boundary conditions and any local perturbation spreads immediately all over the numerical domain. Spectral methods are specially suited for elliptic equations: they allow to put the outer boundary very far away, even at infinity, where one can set up very reliable boundary conditions, and they usually provide smooth and accurate solutions without consuming too much computational resources.
- Evolution equations (2.60), on the contrary, are more close to the hyperbolic type (exemplified by the wave equation), in the sense that local perturbations propagate over the numerical domain with some finite characteristic speed. This allows the appearance of non-smooth profiles, even weak solutions, that are hard to deal with using spectral methods. Either finite difference or finite volume methods are most commonly used with hyperbolic equations, excepting the cases in which only smooth profiles are expected to appear.
- There is no generic way of algebraically splitting the dynamical degrees of freedom in order to single out the ones corresponding to gravitational radiation. As we will see in the next section, such an algebraic splitting can only be done if one knows in advance the gravitational waves propagation direction. This could be the case in highly symmetrical cases: the gravitational radiation degrees of freedom can be actually neglected in the spherical case, so that the radial direction could be used in problems with approximate spherical symmetry. But there is no such rule for the generic case that could be used in a general purpose numerical code.

The obvious alternative to the constrained evolution approach is to use just the six evolution equations (2.60) to compute everything. The constraints

(2.61) and (2.62) could be enforced just on the initial and boundary data, because they are first integrals of the evolution system and this would be enough to ensure their validity inside the computational domain. The constraints provide just a quality check of the calculations. One can even add some 'damping terms,' devised for minimizing constraint violations [13]. This approach, named 'free evolution' [14], continues to be by far the most commonly used in numerical relativity codes, usually implemented with either finite differences or finite elements discretization. This approach has very deep theoretical and practical implications, which will be discussed thoroughly in the next chapter.

2.4 Gravitational waves degrees of freedom

Gravitational waves constitute one of the most outstanding predictions of Einstein's general relativity. One can derive it by standard methods, in the same way as electromagnetic radiation can be derived from Maxwell's equations. The simplest way is to study small field perturbations around a fixed background, along the lines discussed in Sect. 1.4.2. Relativity textbooks usually assume the harmonic gauge, taking the relaxed system (1.65) as the starting point. This is a little bit misleading, because in that way all metric components seem to generate waves, propagating with light speed. Both the harmonic constraints and the residual gauge freedom must be used in order to isolate the true (just two) gravitational wave degrees of freedom.

We will rather follow here a 3+1 approach, so that both the gauge effects and the constraint degrees of freedom are more easily identified. In this way, we will also gain some insight on the structure of the field equations.

2.4.1 Linearized field equations

Let us come back to the full set (evolution plus constraints) of 3+1 equations (2.51), (2.52), (2.53), and (2.54). To avoid coordinate complications, we will choose here Gauss coordinates, that is, normal coordinates (zero shift) and Geodesic slicing (with $\alpha = 1$), so that

$$ds^2 = -dt^2 + \gamma_{ij}\, dx^i\, dx^j\,. \tag{2.73}$$

As discussed in the previous chapter, any metric can be written down at a given spacetime point P in a locally inertial coordinate system such that the first derivatives of the metric coefficients vanish at P. Then, as we can get as close as we want to P, we can safely split the space metric in (2.73) into two components:

- An Euclidean (flat) background of the form

$$\alpha_{(0)} = 1\,, \qquad \gamma^{(0)}_{ij} = \delta_{ij}\,. \tag{2.74}$$

- A linear perturbation which, when superimposed to the background, allows one to recover the full metric

$$\delta\gamma_{ij} = \gamma_{ij} - \gamma^{(0)}_{ij}\,. \tag{2.75}$$

For further convenience, we will relax here the geodesic slicing condition, allowing also for linear perturbations of the lapse function, namely

$$\delta\alpha = \alpha - \alpha_{(0)}. \tag{2.76}$$

Of course, if the extrinsic curvature can be obtained from the first time derivative of the space metric, one must have for consistency

$$K^{(0)}_{ij} = 0\,, \qquad \delta K_{ij} = K_{ij}\,. \tag{2.77}$$

We can substitute the perturbations (2.75), (2.76), and (2.77) into the 3+1 equations (2.51), (2.52), (2.53), and (2.54) for the vacuum case. We get, up to the linear order

$$\partial_t\,(\delta\gamma_{ij}) = -2\,(\delta K_{ij}) \tag{2.78}$$
$$\partial_t\,(\delta K_{ij}) = -\partial^2_{ij}\,(\delta\alpha) + \delta R_{ij} \tag{2.79}$$
$$0 = \delta^{rs}[\partial_r\,(\delta K_{si}) - \partial_i\,(\delta K_{rs})] \tag{2.80}$$
$$0 = tr\,(\delta R)\,, \tag{2.81}$$

where the trace is computed with the flat background metric (2.74) and the linear order expression for the Ricci tensor is given by

$$\delta R_{ij} = -\frac{1}{2}\,\delta^{rs}[\partial^2_{rs}(\delta\gamma_{ij}) + \partial^2_{ij}(\delta\gamma_{rs}) - \partial^2_{ir}(\delta\gamma_{js}) - \partial^2_{jr}(\delta\gamma_{is})]\,. \tag{2.82}$$

2.4.2 Plane-wave analysis

In order to fully analyze the linear system ((2.78), (2.79), (2.80), and (2.81)), it is convenient to Fourier transform the local perturbation and look at the behavior of a generic plane-wave component, propagating along a given direction n_i, namely

$$\delta\alpha = e^{i\,\omega\cdot x}\,a(\omega,t) \tag{2.83}$$
$$\delta\gamma_{ij} = e^{i\,\omega\cdot x}\,h_{ij}(\omega,t) \tag{2.84}$$

$$\delta K_{ij} = e^{i\,\omega\cdot x}\, k_{ij}(\omega, t)\,, \tag{2.85}$$

where $\omega_k = \omega\, n_k$, $\delta^{\,ij}\, n_i\, n_j = 1$.

Now we can translate the partial differential equations system (2.78), (2.79), (2.80), and (2.81) into the following ordinary differential equations system:

$$\partial_t\ h_{ij} = -2\ k_{ij} \tag{2.86}$$

$$\partial_t\ k_{ij} = \omega^2/2\ [\, h_{ij} - n_i\, h_{nj} - n_j\, h_{ni} + (tr\, h + 2\, a)\, n_i\, n_j\,] \tag{2.87}$$

$$0 = k_{ni} - n_i\, tr\, k \tag{2.88}$$

$$0 = tr\, h - h_{nn}\,, \tag{2.89}$$

where the symbol n replacing an index means contraction with n_i. It is then useful to decompose the Fourier modes into longitudinal (aligned with the propagation direction n_i) and transverse components (tangent to the wavefronts, which are the surfaces orthogonal to n_i). One gets then three different types of modes, according to their time evolution:

- Three **static** modes, as we get from (2.88):

$$\partial_t\ (h_{ni} - n_i\, tr\, h) = -2\ (k_{ni} - n_i\, tr\, k) = 0. \tag{2.90}$$

- One **gauge** mode, whose evolution is fully determined by lapse perturbations,

$$\partial_t\ tr\, h = -2\ tr\, k\,, \qquad \partial_t\ tr\, k = \omega^2\, a\,, \tag{2.91}$$

  where we have used (2.89).
- Two **wave** modes, oscillating with the Fourier frequency ω,

$$\partial_t\, h_{\perp\perp} = -2\ k_{\perp\perp}\,, \qquad \partial_t\, k_{\perp\perp} = \omega^2/2\ h_{\perp\perp}\,, \tag{2.92}$$

  where the symbol $\perp$ replacing an index means the projection orthogonal to n_i. There are only two independent modes in (2.92), because the trace part vanishes if we allow for (2.89), that is,

$$tr\,(h_{\perp\perp}) = tr\ h - h_{nn} = 0\,. \tag{2.93}$$

  This static mode was already included in (2.90).

Let us focus in the gauge mode (2.91) for a while. In the Gauss coordinate system no lapse perturbations are allowed ($a = 0$). This means that the equations allow then for a linear growth of the trace $tr\, h$ of the metric perturbation, which corresponds to the linear term of the space metric determinant, namely

$$\gamma \equiv det(\gamma_{ij}) \simeq 1 + e^{i\,\omega\cdot x}\,(tr\, h + \cdots), \tag{2.94}$$

so that the first equation in (2.91) corresponds to the evolution of the space volume element $\sqrt{\gamma}$

$$\partial_t \sqrt{\gamma} = -\alpha \, tr \, K, \tag{2.95}$$

and the linear gauge mode corresponds then to an overall expansion (or collapse) of the space metric. This is one of the main reasons why geodesic slicing is not suitable for numerical simulations, because discretization errors coupled with the gauge mode can produce an artificial linear growing which is easily amplified by the non-linear terms, leading to a numerical blowup. This is why we have relaxed this condition to allow for generic gauge perturbations.

A much suitable choice in this context would be instead the 'maximal slicing' condition [15],

$$tr \, K = 0 \, , \tag{2.96}$$

which ensures that the gauge modes are also static ($\partial_t \, tr \, h = 0$). The time evolution of $tr \, K$ is given by (2.41), so that the maximal slicing condition is preserved if and only if the lapse function verifies the consistency condition

$$\frac{1}{\alpha} \, \triangle \alpha = tr(K^2) + 4\pi \, (trS + \tau) \, , \tag{2.97}$$

which reduces to the Laplace equation, up to the linear order, in the vacuum case.

Maximal slicing has been widely used in numerical relativity codes [16–18], leading to smooth and stable lapse profiles at the cost of solving the elliptic (Laplace-like) equation (2.97) at every time step. In the non-vacuum case, (2.97) reduces at the linear order to the Poisson-like equation

$$\triangle(\delta\alpha) = 4\pi \, \rho \, , \tag{2.98}$$

where we have considered the mass density ρ as the first-order contribution to the energy density τ (this amounts to considering kinetic and pressure effects as higher order terms). This is precisely the field equation in Newtonian gravity

$$\triangle \, \phi = 4\pi \, \rho \, , \tag{2.99}$$

which determines the gravitational potential ϕ for a given mass distribution.

It follows that the lapse perturbation $\delta\alpha$ can be identified with the gravitational potential ϕ in the Newtonian limit. This is consistent if we define the Newtonian limit by the following two conditions:

- We consider perturbations of the Minkowski background up to the linear order.
- We ignore any evolution effect (apart from the ones produced by the motion of the sources): this means neglecting gravitational waves, but also enforcing maximal slicing, as we have seen.

This explains why the maximal slicing condition (2.97) is so effective in providing smooth lapse profiles, independently of the riddles produced by time evolution in other field components.

2.4.3 Gravitational waves and gauge effects

Let us summarize now some results from the previous analysis. If we use normal coordinates with maximal slicing, then, up to the linear order, the only dynamical effects on every Fourier component are the ones described by the two transverse traceless degrees of freedom given by

$$\partial_t \, < h_{\perp\perp} >= -2 \, < k_{\perp\perp} > , \quad \partial_t \, < k_{\perp\perp} >= \omega^2/2 \, < h_{\perp\perp} > , \tag{2.100}$$

where we have noted by $< \cdots >$ the traceless part, for instance,

$$< k_{\perp\perp} > \equiv \, k_{\perp\perp} - \frac{1}{2} \, tr \, (k_{\perp\perp}) \, \delta_{\perp\perp} \, . \tag{2.101}$$

Equations (2.100) imply that the dynamical behavior of the selected Fourier component can be described as the one of a plane wave propagating with the speed of light along the selected direction n_i, that is,

$$\delta \, K_{ij} \sim e^{i \, \omega (n \cdot x \, \pm \, t)} \, . \tag{2.102}$$

From the physical point of view, it follows that gravitational waves should be transverse and traceless and should propagate with light speed. One could wonder whether the fact that gravitational radiation consists of two degrees of freedom could be anticipated by the following naive balance: six components in K_{ij} minus four constraints give precisely two 'gravitational radiation' components.

The fallacy in this argument can be easily discovered if one tries to apply it to Maxwell equations (2.1), (2.2), (2.3), and (2.4). There we have six components in the electric and magnetic fields, minus two constraints, so that four components are left. But electromagnetic radiation has only one degree of freedom. This means that there are non-radiative dynamical contributions to the electromagnetic field that contribute to the linear order. The true balance should read six electromagnetic field components minus two constraints give four dynamical degrees of freedom, but only one of them is of a radiative type. In Einstein's equations, instead, non-radiative dynamical effects do not show up at the linear order, where we just find gravitational radiation, aside from eventual gauge effects.

We have found one such gauge effect: the linear mode (2.91) that appears when using geodesic slicing. Another kind of gauge effect would show up when the time coordinate is given by a harmonic function (harmonic slicing), that is,

$$\Box \, x^0 = 0 \; \longleftrightarrow \; \widehat{\Gamma}^{\, 0} = 0 \, . \tag{2.103}$$

In normal coordinates (zero shift), this amounts to

$$\partial_t \, (\alpha / \sqrt{\gamma}) = 0 \, . \tag{2.104}$$

The gauge perturbation $\delta\alpha$ is then dynamically related with the space volume perturbation. In Fourier space we have

$$\partial_t \ (a - tr\, h) = 0, \tag{2.105}$$

and the gauge mode (2.91) can be written as

$$\partial_t \ a = -tr\, k\,, \qquad \partial_t \ tr\, k = \omega^2\, a\,, \tag{2.106}$$

which reproduces the same propagation behavior as that of gravitational waves

$$\delta\alpha \sim e^{i\,\omega(n\cdot x \pm t)}\,. \tag{2.107}$$

These 'gauge waves' do not describe any physical effect: they are rather an artifact of the gauge choice. We have introduced the harmonic slicing here mainly for two reasons:

- It provides an oscillatory gauge behavior that is between the linear one of geodesic slicing and the static one of maximal slicing. We will use a generalization of this condition in the next chapter in order to obtain hyperbolic evolution systems with a view to numerical simulations.
- The direct relationship (2.103) between the lapse function and the space volume element can be used to avoid collapse singularities in numerical simulations of black hole spacetimes (singularity avoidance, see Fig. 2.2). As we will see later, however, the singularity avoidance behavior of the harmonic slicing gauge is just marginal, so that some stronger singularity-avoidant condition is required for these extreme gravitational collapse scenarios.

References

1. G. Darmois, *Les equations de la Gravitation Einsteinnienne*, Memorial des Sciences Mathematiques **25**, Gauthier-Villars, Paris (1927).
2. A. Lichnerowicz, J. Math. Pures et Appl. **23**, 37 (1944).
3. Y. Choquet-Bruhat, J. Rat. Mec. Anal. **5**, 951 (1956).
4. A. Lichnerowicz, *Studies in the History of General Relativity Series: Einstein Studies*, Vol 3, ed. by J. Eisenstead and A. J. Kox, Birkhäuser, Basel (1992).
5. R. Arnowit, S. Deser and C. W. Misner. *Gravitation: An Introduction to Current Research*, ed. by L. Witten, Wiley, New York (1962). gr-qc/0405109.
6. R. Gomez et al., Phys. Rev. Lett. **80**, 3915 (1998).
7. M. Campanelli, C. O. Lousto, P. Marronetti and Y. Zlochower, Phys. Rev. Lett. **96**,111101 (2006).
8. J. G. Baker et al., Phys. Rev. Lett. **96**, 111102 (2006).
9. M. Alcubierre and B. Brügmann, Phys. Rev. **D63**, 104006 (2001).
10. M. Alcubierre et al., Phys. Rev. **D67**, 084023 (2003).
11. L. Lindblom and M. A. Scheel, Phys. Rev. **D67**, 124005 (2003).
12. F. Pretorius, Phys. Rev. Lett. **95**, 121101 (2005).

13. C. Gundlach, G. Calabrese, I. Hinder and J. M. Martín-García, Class. Quantum Grav. **22**, 3767 (2005).
14. J. Centrella, Phys. Rev. **D21**, 2776 (1980).
15. F. Estabrook et al., Phys. Rev. **D7**, 2814 (1973).
16. L. Smarr and J. W. York, Phys. Rev. **D17**, 1945 (1978).
17. L. Smarr and J. W. York, Phys. Rev. **D17**, 2529 (1978).
18. P. Anninos et al., Phys. Rev. Lett. **71**, 2851 (1993).

http://www.springer.com/978-3-642-01163-4

Elements of Numerical Relativity and Relativistic Hydrodynamics

From Einstein' s Equations to Astrophysical Simulations

Bona, C.; Palenzuela-Luque, C.; Bona-Casas, C.

2009, XIV, 214 p. 108 illus., Hardcover

ISBN: 978-3-642-01163-4